universe

MDPI

Review

Neutron Dark Decay

Bartosz Fornal

Department of Chemistry and Physics, Barry University, Miami Shores, FL 33161, USA; bfornal@barry.edu

Abstract: There exists a puzzling disagreement between the results for the neutron lifetime obtained in experiments using the beam technique versus those relying on the bottle method. A possible explanation of this discrepancy postulates the existence of a beyond-Standard-Model decay channel of the neutron involving new particles in the final state, some of which can be dark matter candidates. We review the current theoretical status of this proposal and discuss the particle physics models accommodating such a dark decay. We then elaborate on the efforts undertaken to test this hypothesis, summarizing the prospects for probing neutron dark decay channels in future experiments.

Keywords: neutron lifetime anomaly; dark matter; physics beyond the Standard Model

1. Introduction

Almost all of the visible matter in the Universe is made up of atoms, which consist of electrons, protons, and neutrons. This picture of the subatomic world emerged only less than a century ago. The electron was discovered by Joseph Thomson in 1897 [1], whereas the proton was proposed by Ernest Rutherford in 1919 [2]. The first hints of the existence of a neutron were provided by Irène Joliot-Curie and Frédéric Joliot-Curie in early 1932 [3], but the actual proposal supported by further experiments was put forward by James Chadwick later in 1932 [4]. Soon afterwards, Irène and Frédéric Joliot-Curie precisely determined the mass of the neutron [5], identifying it to be heavier than the proton. This mass relation allows the neutron to decay and has profound implications for the physics at the nuclear level.

Due to nonzero binding energy inside a nucleus, the neutron does not decay in stable nuclei. However, on its own, it undergoes a β decay predominantly to a proton, electron, and electron antineutrino (see Figure 1),

$$n \to p + e + \bar{\nu}_e \, . \tag{1}$$

Apart from this leading order process, there are channels involving photons in the final state with a branching ratio $\mathrm{Br}(n \to p + e + \bar{\nu}_e + \gamma) \sim 1\%$ [6]. Finally, there exists also a decay channel to hydrogen and an antineutrino, but the corresponding branching ratio is tiny, $\mathrm{Br}(n \to \mathrm{H} + \bar{\nu}_e) \sim 4 \times 10^{-6}$ [7].

A precise calculation of the neutron lifetime within the framework of the Standard Model [8–15], taking into account radiative corrections, yields the formula [16,17]

$$\tau_n = \frac{4908.6(1.9)\ \mathrm{s}}{(1+3\lambda^2)|V_{ud}|^2} \, , \tag{2}$$

where λ is the ratio of the axial-vector current coefficient and the vector current coefficient in the matrix element for the neutron β decay,

$$\mathcal{M} = \frac{G_F}{\sqrt{2}} V_{ud}\, g_V \left[\, \bar{p}\, \gamma_\mu n - \lambda\, \bar{p}\, \gamma_5 \gamma_\mu n \,\right] \left[\, \bar{e}\, \gamma^\mu (1-\gamma_5) \nu \,\right], \tag{3}$$

Citation: Fornal, B. Neutron Dark Decay. *Universe* **2023**, *9*, 449. https://doi.org/10.3390/universe9100449

Academic Editor: Ignazio Bombaci

Received: 28 June 2023
Revised: 9 October 2023
Accepted: 11 October 2023
Published: 16 October 2023

and V_{ud} is the Cabibbo–Kobayashi–Maskawa (CKM) matrix element, which, based on the 15 most precisely measured superallowed transitions [18], has a dispersion-relation-based weighted average of $|V_{ud}| = 0.97373(11)(9)(27)$ [19]. Using the up-to-date average for the ratio of the axial-vector to vector current coefficient, $\lambda_{\rm av} = -1.2754 \pm 0.0013$ [19], the resulting neutron lifetime from Equation (2) is $\tau_n = 880.5 \pm 2.3$ s. An independent nuclear lattice calculation gives $\lambda_{\rm lattice} = -1.271 \pm 0.013$ [20], which corresponds to $\tau_n = 885 \pm 15$ s.

Due to difficulties in isolating low-energy neutrons, experiments capable of directly measuring the neutron lifetime were not performed until fairly recently. At present, there are two qualitatively different techniques implemented to perform this measurement: the beam method and the bottle method. For a review of those methods, including a detailed timeline of neutron lifetime measurements for each of them, see [21,22].

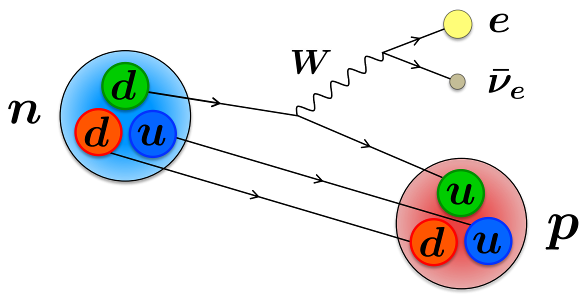

Figure 1. Dominant neutron decay $n \to p + e + \bar{\nu}_e$ in the Standard Model.

In beam experiments [23–26], a collimated beam of cold neutrons passes through a quasi-Penning trap. The protons from neutron decays are trapped and counted, enabling the determination of the rate of neutron decays involving protons in the final state, dN_p/dt. The flux of neutrons in the beam is found by counting α particles and tritium nuclei from the (n, α) reaction in a deposit of ^{6}LiF on a thin silicon crystal wafer, and the number of neutrons, N_n, from which the trapped protons originated is established. The beam neutron lifetime is then calculated as

$$\tau_n^{\rm beam} = -N_n \left(\frac{dN_p}{dt} \right)^{-1} . \tag{4}$$

In the bottle method, ultracold neutrons (UCN) are loaded into a specially prepared container (either a material bottle [27–31] or a magnetic bottle [32–34]), stored for varying times, and the surviving UCN are emptied and counted using, e.g., a ^{3}He proportional counter, thus determining N_n as a function of time. Since the decay pattern is exponential, the bottle neutron lifetime is obtained from the fit to the experimental points of the function

$$N_n(t) = N_0 \exp\Big(-t/\tau_n^{\rm bottle}\Big) . \tag{5}$$

Figure 2 presents a summary of the recent neutron lifetime measurements, including the available beam experiment results [23–26] and bottle experiment results [27–34]. There is a clear mismatch between the two types of measurements. The average neutron lifetime from the beam experiments [23,25] is

$$\tau_n^{\rm beam} = 888.0 \pm 2.0 \text{ s} , \tag{6}$$

while the average from bottle experiments is

$$\tau_n^{\rm bottle} = 878.4 \pm 0.5 \text{ s} . \tag{7}$$

The discrepancy is at the level of four standard deviations. Although this might be due to systematic errors that are unaccounted for, some sort of new physics affecting the way neutron decays is a viable possibility to consider.

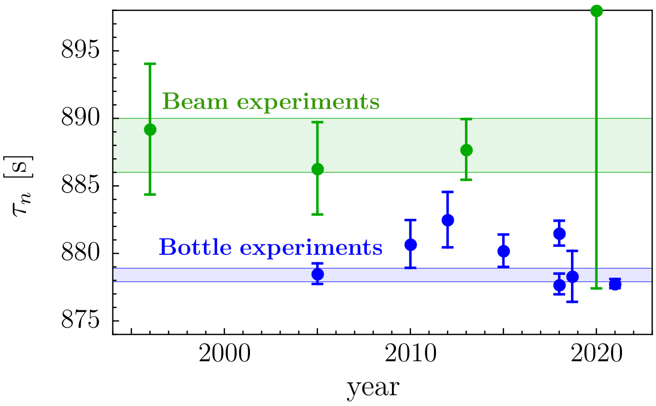

Figure 2. Neutron lifetime measurements in beam experiments (green) [23–26] and bottle experiments (blue) [27–34] over the last 30 years. The 2013 beam result is based on a reanalysis of the 2005 data.

Since in the Standard Model, one always expects a proton in the final state of neutron decay, the beam and bottle experiments should give the same result, with just a tiny difference due to the decay channel $n \to \mathrm{H} + \bar{\nu}_e$ (the beam experiment is not sensitive to it). Therefore, within the Standard Model, one has $\mathrm{Br}(n \to p + \text{anything})_{\mathrm{SM}} = 1$ with accuracy $\mathcal{O}(10^{-5})$.

The crucial observation is that one can reconcile the results in Equations (6) and (7) if the neutron has one or more extra decay channels for which none of the final state particles is a proton. Indeed, since the beam method is not sensitive to them, the beam and bottle lifetimes are related by

$$\tau_n^{\text{bottle}} = \tau_n^{\text{beam}} \times \mathrm{Br}(n \to p + \text{anything}) \leq \tau_n^{\text{beam}} \,, \tag{8}$$

so, in the presence of protonless neutron decay channels, it is possible to have a relation between the two measurement of the form $\tau_n^{\text{bottle}} < \tau_n^{\text{beam}}$, exactly as the current beam and bottle results suggest.

More precisely, if the branching ratio for neutron beta decays is

$$\mathrm{Br}(n \to p + \text{anything}) \approx 99\% \,, \tag{9}$$

and the remaining channels corresponds to beyond-Standard-Model neutron dark decays not involving a proton in the final state,

$$\mathrm{Br}(n \to \text{anything} \neq p) \approx 1\% \,, \tag{10}$$

the two experimental results remain consistent with each other. This lies at the heart of the idea proposed in [35], where phenomenologically viable extensions of the Standard Model were constructed with Equations (9) and (10) satisfied, as summarized below.

The plan for the review is as follows: In Section 2, we analyze the neutron dark decay scenario at the effective field theory level, deriving the general conditions that the corresponding models need to satisfy, and we discuss the various possible final states. In Section 3, we construct concrete particle physics models with neutron dark decays occurring at a branching ratio of 1%, which are consistent with all other experiments. In Section 4, we discuss the progress made on the experimental side to test the neutron dark decay proposal, and in Section 5, we elaborate on the theoretical developments in this area, including those connecting neutron dark decay to other open questions in particle physics. A brief summary and conclusions are presented in Section 6.

2. Effective Picture of Neutron Dark Decay

Here, we review the model-independent requirements that theories involving neutron dark decays need to satisfy to be phenomenologically acceptable. We are considering the neutron decaying to two or more particles, at least one of which is a new (dark) particle from outside of the Standard Model, hence the name *neutron dark decay*. In the most interesting scenarios, one or several of those dark particles are viable dark matter candidates.

2.1. Stability of Nuclei

Let us denote the final state of neutron dark decay by f and the sum of final state particle masses by M_f. This sum obviously cannot be heavier than the neutron itself; thus, $M_f < m_n$. It also cannot be too small, since otherwise, stable nuclei would undergo dark decays, contrary to what is observed. The lower bound can be derived through the following simple reasoning.

If in a nucleus with atomic number Z and mass number A one of its neutrons underwent a dark decay, this would lead to $(Z, A) \to (Z, A-1)^* + f$. The final state excited nucleus $(Z, A-1)^*$ would then de-excite emitting secondary particles, mostly photons. However, such signatures were looked for at the Sudbury Neutrino Observatory (SNO) [36] and at the Kamioka Liquid Scintillator Antineutrino Detector [37] and none were discovered. As a result, those searches placed a lower bound on the neutron lifetime from such generic *nuclear dark decays* of $\tau_n \gtrsim 6 \times 10^{29}$ years, obviously ruling out neutron dark decays with a branching ratio of 1%.

However, there exists a nonzero parameter space for which nuclear dark decays are forbidden despite the neutron on its own still undergoing dark decays. The mechanism behind this is identical to the standard one which prevents stable nuclei from decaying despite the neutron itself undergoing β decay. Indeed, if the following mass relation holds,

$$m_n - S_n < M_f < m_n \,, \tag{11}$$

where S_n is the separation energy for a neutron in the nucleus, then the nuclear dark decay $(Z, A) \to (Z, A-1)^* + f$ is kinematically forbidden, while the neutron can still undergo a dark decay when by itself. The most stringent constraint in Equation (11) is provided by the stable nucleus which has the lowest neutron separation energy—this happens to be beryllium-9 with $S_n(^9\mathrm{Be}) = 1.664$ MeV. Actually, a slightly stronger bound applies in this case, since a ^{9}Be decay would proceed via $^9\mathrm{Be} \to {}^8\mathrm{Be}^* + f \to 2\alpha + f$ due to a rapid disintegration of excited beryllium-8 to two αparticles, lowering the threshold for the nuclear dark decay by $\sim$93 keV [38]. Taking this into account, the constraint becomes

$$937.993 \text{ MeV} < M_f < 939.565 \text{ MeV} \,. \tag{12}$$

This relation assures also the stability of the proton, which would otherwise undergo dark decays via $p \to f + e^+ + \nu_e$ if $M_f < m_p - m_e = 937.761$ MeV.

Intriguingly, there exist unstable nuclei whose decay patterns might be affected by neutron dark decays, since those decays are allowed if the neutron separation energy for unstable nuclei is $S_n < 1.572$ MeV. Searches for such nuclear dark decays will be discussed in Section 4.

2.2. Neutron Dark Decay Channels

The fact that neutron dark decays are phenomenologically viable when the relation in Equation (12) holds opened the gates to entirely new model-building opportunities not considered before. As mentioned earlier, the new neutron decay channels involve at least one beyond-Standard-Model particle in the final state. Those new particles can be either fermions (denoted by χ) or bosons (scalars denoted by ϕ and vectors denoted by V). The simplest possible dark decay channels for the neutron include the following:

$$n \to \chi\,\gamma\,, \quad n \to \chi\,\phi\,, \quad \ldots \quad, \tag{13}$$

where the decays not written out explicitly can include other dark particles, photons, neutrinos, and electrons/positrons in the final state.

In an effective Lagrangian picture of neutron dark decays, the process is governed by the mixing term between the neutron and the dark fermion χ',

$$\mathcal{L}^{\rm eff}_{\rm mix} = \varepsilon\,(\bar{n}\,\chi' + \bar{\chi}'n)\;, \tag{14}$$

where ε is a model-dependent parameter with a dimension of mass. This dark fermion χ' can either be the final state particle χ from the decay $n \to \chi\,\gamma$ or an intermediate fermion $\tilde{\chi}$ allowing for the decay $n \to \chi\,\phi$. Both of those cases are discussed in detail below.

2.3. Neutron $\to$ Dark Fermion + Photon

In the effective field theory picture, the case $n \to \chi\,\gamma$ requires only one new fermion χ. Its mass is constrained by the condition in Equation (12) to satisfy

$$937.993\ \text{MeV} < m_\chi < 939.565\ \text{MeV}\;, \tag{15}$$

thus, the energy of the monochromatic photon in the final state, depending on the mass of χ, takes a value within the range

$$0 < E_\gamma < 1.572\ \text{MeV}\;. \tag{16}$$

In the limit $m_\chi \to m_n$, the energy of the monochromatic photon $E_\gamma \to 0$.

The final state fermion χ, if stable, may be a good dark matter candidate. In that case, to prevent χ from β decaying, one requires

$$937.993\ \text{MeV} < m_\chi < m_p + m_e = 938.783\ \text{MeV}\;, \tag{17}$$

which considerably narrows down the range of the expected photon energies to

$$0.782\ \text{MeV} < E_\gamma < 1.572\ \text{MeV}\;. \tag{18}$$

This very concrete prediction was the trigger for experimentalists to start looking for such a signal immediately after the proposal in [35] was made [39].

A quantitative description of the decay channel $n \to \chi\,\gamma$ is obtained by constructing an effective Lagrangian containing the terms in Equation (14) and the neutron's magnetic moment,

$$\mathcal{L}^{\rm eff}_{I} = \bar{n}\left(i\partial\!\!\!/ - m_n + \frac{g_n e}{8m_n}\sigma^{\mu\nu}F_{\mu\nu}\right)n + \bar{\chi}\left(i\partial\!\!\!/ - m_\chi\right)\chi + \varepsilon(\bar{n}\,\chi + \bar{\chi}\,n), \tag{19}$$

where g_n is the g-factor of the neutron. The rate for the neutron dark decay $n \to \chi\,\gamma$ is

$$\Delta\Gamma_{n\to\chi\gamma} = \frac{g_n^2 e^2}{128\pi}\left(1 - \frac{m_\chi^2}{m_n^2}\right)^3\left(\frac{\varepsilon}{m_n - m_\chi}\right)^2 m_n\;. \tag{20}$$

If $\Delta\Gamma_{n\to\chi\gamma}/\Gamma_n \approx 1\%$, where Γ_n is the total neutron decay rate, this provides a viable explanation for the observed discrepancy between the beam and bottle experiments. The corresponding particle physics framework for this case (Model 1) will be constructed in Section 3.

2.4. Neutron $\to$ Dark Fermion + Dark Scalar

The effective theory for the pure dark decay $n \to \chi\,\phi$ contains two new fermions χ and $\tilde{\chi}$ as well as a new scalar ϕ. In general, the scalar ϕ can be replaced by a vector boson V_μ. The dark fermion $\tilde{\chi}$ is an intermediate particle mixing with the neutron and coupling to χ and ϕ. The sum of masses $m_\chi + m_\phi$ is constrained by the condition in Equation (12) to satisfy

$$937.993 \text{ MeV} < m_\chi + m_\phi < 939.565 \text{ MeV}\,, \tag{21}$$

whereas the mass of $\tilde{\chi}$ is bounded from below, $m_{\tilde{\chi}} > 937.993$ MeV, to prevent the decay of ^{9}Be triggered by the neutron dark decay $n \to \tilde{\chi}\,\gamma$.

The final state fermion χ and scalar ϕ can be dark matter candidates if they are stable, which happens when

$$|m_\chi - m_\phi| < m_p + m_e = 938.783 \text{ MeV}\,. \tag{22}$$

Apart from the relations above, there are no other constraints on the masses m_χ and m_ϕ, e.g., one can have $m_\chi \gg m_\phi$, $m_\chi \ll m_\phi$, or $m_\chi \approx m_\phi$.

The case $n \to \chi\phi$ can be effectively described by the Lagrangian

$$\mathcal{L}_{II}^{\rm eff} \;=\; \mathcal{L}_{I}^{\rm eff}(\chi \to \tilde{\chi}) + (\lambda_\phi\, \bar{\tilde{\chi}}\, \chi\, \phi + \text{h.c.}) + \bar{\chi}\,(i\partial\!\!\!/ - m_\chi)\,\chi \;+ \partial_\mu\phi^*\partial^\mu\phi - m_\phi^2|\phi|^2\,, \tag{23}$$

which results in the neutron dark decay rate

$$\Delta\Gamma_{n\to\chi\phi} = \frac{|\lambda_\phi|^2}{16\pi}\sqrt{[(1+x)^2-y^2][(1-x)^2-y^2]^3}\left(\frac{\varepsilon}{m_n - m_{\tilde{\chi}}}\right)^2 m_n\,, \tag{24}$$

where $x = m_\chi/m_n$ and $y = m_\phi/m_n$. If $m_{\tilde{\chi}} > m_n$, then $n \to \chi\,\phi$ is the only dark decay channel available and provides a solution to the neutron lifetime discrepancy if $\Delta\Gamma_{n\to\chi\phi}/\Gamma_n \approx 1\%$. However, if $m_n > m_{\tilde{\chi}} > 937.993$ MeV, then an additional dark decay channel opens up, $n \to \tilde{\chi}\,\gamma$, with a decay rate $\Delta\Gamma_{n\to\tilde{\chi}\gamma} = \Delta\Gamma_{n\to\chi\gamma}(m_\chi \to m_{\tilde{\chi}})$. If the following relation is satisfied,

$$\left(\Delta\Gamma_{n\to\chi\phi} + \Delta\Gamma_{n\to\tilde{\chi}\gamma}\right)/\Gamma_n \approx 1\%\,, \tag{25}$$

this also explains the discrepancy between the beam and bottle experiments. The corresponding particle physics model in this case is constructed below (Model 2). We note that this picture can be further simplified if the fermion χ also plays the role of the intermediate particle $\tilde{\chi}$.

3. Particle Physics Models

In this section, we discuss the two simplest microscopic renormalizable models providing realizations of the neutron dark decay cases $n \to \chi\,\gamma$ and $n \to \chi\,\phi$. Those models were constructed in [35], but it was later shown that consistency with the observed neutron star masses requires additional interactions to be present, which we will review in Section 5.

3.1. Model 1

The minimum number of new fields needed at the particle physics level to realize the neutron dark decay $n \to \chi\,\gamma$ is two: the Standard Model singlet Dirac fermion χ in the final state discussed earlier and a color triplet scalar $\Phi = (3,1)_{-1/3}$ producing the mixing terms in Equation (14) between the neutron and χ. The Lagrangian for such a theory includes

$$\mathcal{L}_1 \;\supset\; \lambda_q \epsilon^{ijk}\overline{u^c_{L}}_i d_{Rj}\Phi_k + \lambda_\chi \Phi^{*i}\bar{\chi}\, d_{Ri} \;+\; \text{h.c.}\,, \tag{26}$$

where the superscript c denotes charge conjugation. It is possible to define a conserved generalized baryon number B if one assigns $B_\chi = 1$, $B_\Phi = -2/3$, and the standard $B_q = 1/3$ to the quarks.

Figure 3 shows a schematic diagram of the neutron dark decay $n \to \chi\,\gamma$ in Model 1. Upon matching the effective Lagrangian in Equation (19) with the particle-level Lagrangian in Equation (26), the decay rate is given by Equation (20) with

$$\varepsilon = \beta\,\lambda_q \lambda_\chi / m_\Phi^2\,, \tag{27}$$

where $\beta = 0.0144(3)(21)\ \mathrm{GeV}^3$ is determined from a lattice calculation [40].

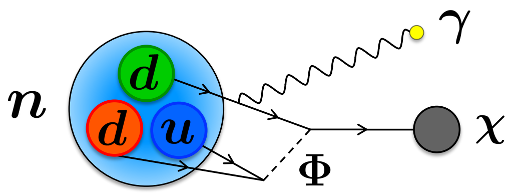

Figure 3. Neutron dark decay $n \to \chi\,\gamma$ in Model 1.

The required neutron dark decay rate of $\Delta\Gamma_{n\to\chi\gamma}/\Gamma_n \approx 1\%$ is achieved for phenomenologically viable values of model parameters. In particular, setting $m_\chi \approx 938$ MeV, i.e., at its minimal value given the requirement in Equation (15), the particle physics parameter choice leading to the 1% branching ratio is

$$m_\Phi \approx (200\ \mathrm{TeV})\sqrt{|\lambda_q \lambda_\chi|}\,. \tag{28}$$

All collider bounds are satisfied for $m_\Phi \gtrsim 1$ TeV, while the dinucleon decay [41] and neutron–antineutron oscillation [42] constraints do not apply, since χ is a Dirac fermion with nonzero baryon number.

3.2. Model 2

For the decay $n \to \chi\phi$ to take place, four new fields at the particle physics level are introduced: Standard Model singlet Dirac fermions χ, $\tilde{\chi}$, scalar ϕ, and the same color triplet scalar $\Phi = (3,1)_{-1/3}$ as in Model 1. The corresponding Lagrangian contains the terms

$$\mathcal{L}_2 \supset \lambda_q \epsilon^{ijk} \overline{u^c_{Li}} d_{Rj} \Phi_k + \lambda_{\tilde{\chi}} \Phi^{*i} \bar{\tilde{\chi}}\, d_{Ri} + \lambda_\phi \bar{\tilde{\chi}}\,\chi\,\phi \;+\; \mathrm{h.c.}\,. \tag{29}$$

The baryon number is again conserved if $B_\phi = 0$, $B_{\tilde{\chi}} = B_\chi = 1$, and $B_\Phi = -2/3$.

Figure 4 shows a schematic diagram of the neutron dark decay $n \to \chi\,\phi$ in Model 2. Comparing the Lagrangians in Equations (23) and (29), the matching procedure yields the decay rate given by Equation (24) with $\varepsilon = \beta\,\lambda_q \lambda_{\tilde{\chi}} / m_\Phi^2$. The required decay rate of $\Delta\Gamma_{n\to\chi\phi}/\Gamma_n \approx 1\%$ is achieved for many parameter choices, e.g., $m_\chi = 938$ MeV, $m_\phi \ll m_\chi$, $m_{\tilde{\chi}} = 2\,m_n$, and

$$m_\Phi \approx (300\ \mathrm{TeV})\sqrt{|\lambda_q \lambda_{\tilde{\chi}} \lambda_\phi|}\,, \tag{30}$$

again remaining consistent with experimental constraints, to simplify the model even further, the intermediate fermion $\tilde{\chi}$ can be taken to be the same χ particle that appears in the final state of neutron dark decay.

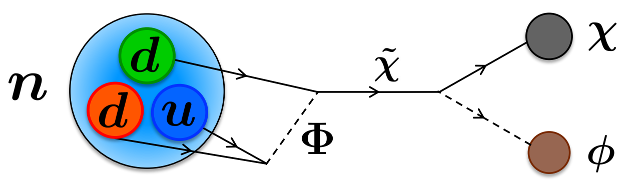

Figure 4. Neutron dark decay $n \to \chi\,\phi$ in Model 2.

4. Experimental Progress

Searches for signatures of neutron dark decay were initiated right after the neutron dark decay proposal in [35] was put forward. They involved looking for the photon from neutron dark decays $n \to \chi\,\gamma$, the electron–positron pair from $n \to \chi\,e^+e^-$, and nuclear dark decay signatures triggered by $n \to \chi\,\phi$. In addition, several new search strategies have been proposed to look for signs of neutron dark decay in other ongoing and future experiments.

4.1. Search for $n \to \chi\,\gamma$

A dedicated experiment searching for the monochromatic photon from the neutron dark decay $n \to \chi\,\gamma$ was carried out at the Ultracold Neutron (UCN) facility at Los Alamos [39] within a few weeks after the idea in [35] was proposed. It was sensitive to photon energies 0.782 MeV $< E_\gamma <$ 1.664 MeV, thus covering the entire range expected if χ is a dark matter candidate. The results were negative and excluded a dark decay branching ratio of $\mathrm{Br}(n \to \chi\,\gamma) = 1\%$ at a significance of 2.2 standard deviations.

Further analysis of these data was carried out in [43], where more detailed bounds on the $n \to \chi\,\gamma$ decay channel were derived as a function of the χ mass (see Figure 5). The green-shaded region corresponds to the parameter space ruled out by the UCN experiment [39] at a 90% confidence level, whereas the purple-shaded region is excluded by the Borexino experiment [44]. It is clear that the neutron dark decay with a branching ratio of 1%, denoted by the black line, is in tension with those results.

In the remaining region of parameter space, where χ is not a dark matter particle, the $n \to \chi\,\gamma$ decay channel is constrained by primordial nucleosynthesis and a cosmic microwave background [45], which are affected by the new decay channel of the neutron and the dark particle, respectively. According to that analysis, a neutron dark decay with a branching ratio of 1% is excluded when $m_\chi \gtrsim 938.9$ MeV.

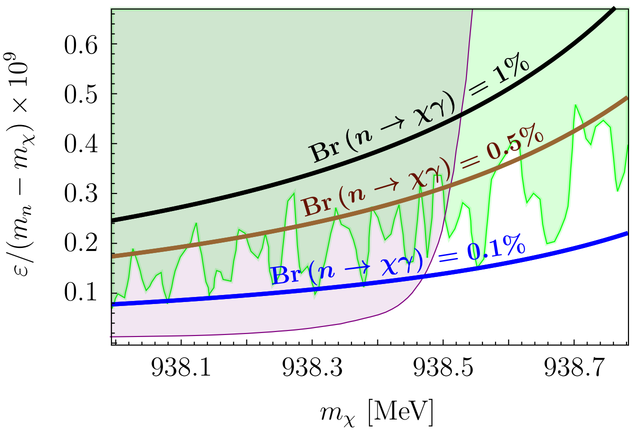

Figure 5. Plot of the parameter space of dark matter mass m_χ versus the mixing $\varepsilon/(m_n - m_\chi)$ with the curves corresponding to the branching ratios for $n \to \chi\,\gamma$ of 1% (black), 0.5% (brown), and 0.1% (blue). The green-shaded region denotes the 90% confidence level exclusion from the Los Alamos UCN experiment [39]; the purple-shaded region corresponds to the exclusion from Borexino [43,44].

4.2. Search for $n \to \chi\,e^+e^-$

One month later, an analysis of another set of Los Alamos UCN data was performed in the search of the electron–positron pairs from the possible neutron dark decay channel $n \to \chi\,e^+e^-$ [46]. However, no e^+e^- pairs were found, and a stringent bound of $(E_{ee} - 2\,m_e) \gtrsim 100$ keV was derived for the branching ratio $\mathrm{Br}(n \to \chi\,e^+e^-) = 1\%$. This constraint was improved the following year by the PERKEO II experiment [47], and a strong exclusion was set for the energy region $(E_{ee} - 2\,m_e) \gtrsim 30$ keV.

4.3. Search for Nuclear Dark Decays

As was shown in Section 2, all stable nuclei are safe from dark decays if the final state of neutron dark decay has a mass $M_f > 937.993$ MeV. This bound is saturated by ^{9}Be, which has the lowest neutron separation energy, $S_n(^9\text{Be}) = 1.664$ MeV, out of all stable nuclei. Nevertheless, many unstable nuclei have neutron separation energies S_n smaller than that of ^{9}Be, which makes dark decays of such nuclei possible if the χ and ϕ particles are sufficiently light, i.e., if the following mass relation holds,

$$937.993 \text{ MeV} < M_f < m_n - S_n \,. \tag{31}$$

An example of such an unstable nucleus is ^{11}Li with a neutron separation energy $S_n(^{11}\text{Li}) = 0.396$ MeV, which was suggested in [35] as a candidate for the nuclear dark decay search. Such a process would lead to

$$^{11}\text{Li} \rightarrow \,^{10}\text{Li}^* + \chi \rightarrow \,^{9}\text{Li} + n + \chi \,. \tag{32}$$

Nevertheless, as pointed out in [38], this signal would be difficult to separate from the β-delayed deuteron emission background.

4.3.1. ^{11}Be Dark Decay

It was also argued in [38] that the ^{11}Be nucleus, characterized by a neutron separation energy of $S_n(^{11}\text{Be}) = 0.502$ MeV, is a much better candidate to look for nuclear dark decays. It has a halo neutron, which enables calculating the rate of ^{11}Be dark decay without the knowledge of nuclear matrix elements. The main decay channels of ^{11}Be are: $^{11}\text{Be} \rightarrow \,^{11}\text{B} + e + \bar{\nu}_e$ and $^{11}\text{Be} \rightarrow \,^{11}\text{B}^* \rightarrow \,^{7}\text{Li} + \,^{4}\text{He} + e + \bar{\nu}_e$ with branching ratios $\sim$97.1% and $\sim$2.9%, respectively. Apart from those, there is also a theoretically expected β-delayed proton emission channel $^{11}\text{Be} \rightarrow \,^{10}\text{Be} + p$ with a branching ratio $\sim 2 \times 10^{-8}$ [48].

Interestingly, in an experiment measuring the number of ^{10}Be nuclei from ^{11}Be decays [49], it was found that there were $\sim$400 times more ^{10}Be nuclei than expected based on the above branching ratio. It was proposed in [38] that this might be explained by the decays

$$^{11}\text{Be} \rightarrow \,^{10}\text{Be} + \chi + \phi \,, \tag{33}$$

which are caused by the halo neutron undergoing the dark decay $n \rightarrow \chi\,\phi$, and it was demonstrated that having $\text{Br}(^{11}\text{Be} \rightarrow \,^{10}\text{Be} + \chi + \phi) \sim 8 \times 10^{-6}$ is consistent within Model 2. Further theoretical work [50] specified that such a dark decay of ^{11}Be is phenomenologically viable if $m_{\tilde{\chi}} > m_n - S_n = 939.064$ MeV. The question was whether there are protons in the final state of ^{11}Be decays. A positive answer would suggest the existence of a near-threshold resonance in ^{11}B emitting protons, whereas a lack of protons would point to a dark decay.

Three collaborations undertook the task of measuring this in four different experiments: one group at CERN–ISOLDE [51], a second group at the Isotope Separator and Accelerator (ISAC) at TRIUMF [52] and at the National Superconducting Cyclotron Laboratory at Michigan State University [53], and a third group at Florida State University [54]. The results of the first group have yet to be published. The results of the ISAC–TRIUMF experiment [52] indicate that the number of protons from ^{11}Be decays roughly matches the number of ^{10}Be nuclei found in [49], thus ruling out neutron dark decays in the mass range $937.993 \text{ MeV} < M_f < 939.064$ MeV and suggesting that the large number of protons observed in [49] was the result of a near-threshold resonance in ^{11}B that enhanced the rate of β-delayed proton emission in ^{11}Be decays. The presence of this resonance was confirmed by the NSCL–MSU experiment [53] and the FSU experiment [54]. Such a resonance was also hinted at by theoretical calculations [55,56]. Nevertheless, a reanalysis of the [49] data discarded the original result and led to an upper bound of

$\text{Br}(^{11}\text{Be} \rightarrow {}^{10}\text{Be} + \text{anything}) \lesssim 2 \times 10^{-6}$ [57] in contradiction with the result of [52], indicating the need for further investigation.

4.3.2. ^{6}He Dark Decay

Another candidate to search for nuclear dark decays is ^{6}He [58], which is a loosely bound unstable nucleus with a two-neutron separation energy of $S_{2n}(^6\text{He}) = 0.975$ MeV. It is energetically forbidden for it to decay via neutron emission. The ground state of ^{6}He decays predominantly via $^6\text{He} \rightarrow {}^6\text{Li} + e + \bar{\nu}_e$, and the only other energetically allowed decay channel is $^6\text{He} \rightarrow {}^4\text{He} + {}^2\text{H}$ with a branching ratio of $\sim 2.78 \times 10^{-6}$ [59–61]. Nevertheless, the ^{6}He nucleus would undergo the dark decay

$$^6\text{He} \rightarrow {}^4\text{He} + n + \chi \tag{34}$$

if the mass of the dark particle χ satisfied the relation

$$937.993 \text{ MeV} < m_\chi < 938.590 \text{ MeV}. \tag{35}$$

This would constitute a very unique signature, i.e., emission of the second neutron, which can be measured with high accuracy. As argued in [38], a successful explanation of the neutron lifetime anomaly requires $\text{Br}(^6\text{He} \rightarrow {}^4\text{He} + n + \chi) \sim 1.2 \times 10^{-5}$.

The experiment searching precisely for this decay channel has recently been performed at the Large Heavy Ion National Accelerator (GANIL) [58]. It resulted in a 95% CL upper limit on the branching ratio of $\text{Br}(^6\text{He} \rightarrow {}^4\text{He} + n + \chi) \leq 4.0 \times 10^{-10}$, which is well below the expected value for the ^{6}He dark decay.

4.4. Beam and Bottle Experiments

Since the neutron lifetime puzzle arises from the discrepancy between two (1996 and 2013) beam results and multiple bottle results, its resolution relies to a large extent on the outcome of the presently operating two beam neutron lifetime experiments: at the National Institute of Standards and Technology (BL2 experiment) [62,63] and at the Japan Proton Accelerator Research Complex [26,64–66]. There is also ongoing work on the improved version of the beam experiment within the BL3 collaboration at NIST [67–70]. We also note that the NIST beam experiment measures protons, whereas J-PARC is sensitive to electrons from neutron β decays, making the two experiments complementary. The initial data from J-PARC reported in [26] are not yet sufficiently precise to favor any of the two results.

Another direct way of probing the neutron lifetime discrepancy is to place a proton counter inside a bottle detector [71], which would enable measuring the decay rate to protons simultaneously with the total neutron decay rate, thus lowering the possibility of unaccounted for systematic errors. This new approach is currently being pursued within the Los Alamos UCN group under the project UCNProBe [72,73].

4.5. Neutron Lifetime from β Decay Parameters

The neutron lifetime in the Standard Model is determined, through the relation in Equation (2), by the V_{ud} element of the CKM matrix and the ratio λ of the axial-vector to vector current coefficients in the β decay matrix element. The value of V_{ud} is measured very accurately in superallowed β decays [18], and its average adopted by the PDG is $|V_{ud}| = 0.97373(11)(9)(27)$ [19]. The most recent precise measurement of λ from the energy spectrum of β decay electrons provided by PERKEO III [74] is

$$|\lambda_{\text{Perkeo III}}| = 1.27641 \pm 0.00045 \pm 0.00033\,. \tag{36}$$

However, the value of λ determined from the energy spectrum of protons measured in the aSPECT experiment [75] is significantly lower,

$$|\lambda_{\text{aSPECT}}| = 1.2677 \pm 0.0028\,. \tag{37}$$

There is also a more recent result from the aCORN experiment [76] extracting λ from the spectrum of electrons, but it has a sizable error, $|\lambda_{\rm aCORN}| = 1.2796(62)$. For more details regarding the β decay parameters, see [77].

Figure 6 displays the parameter space $|\lambda|$ versus $|V_{ud}|$ with the PERKEO III result (brown) and the aSPECT result (orange) overlaid with the bands corresponding to the neutron lifetime beam average (green) from Equation (6), bottle average (blue) from Equation (7), and $|V_{ud}|$ determined from superallowed transitions. The PERKEO III result agrees with the bottle average, but the aSPECT experiment is consistent with the beam average, favoring the neutron dark decay proposal as a solution to the neutron lifetime puzzle.

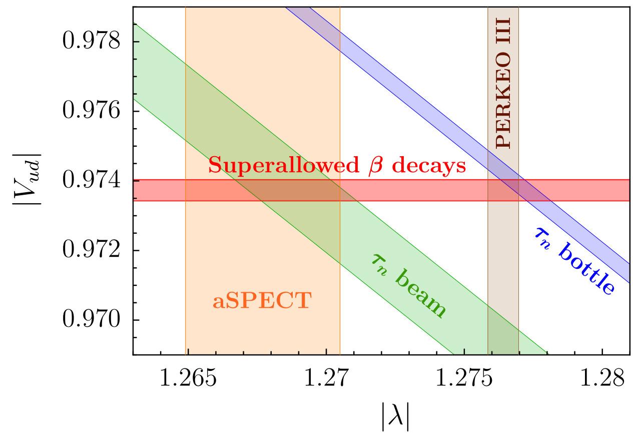

Figure 6. Compilation plot of the $|\lambda|$ vs. $|V_{ud}|$ parameter space regions favored by the neutron lifetime beam average (green), bottle average (blue), superallowed β decays [18,19] (red), PERKEO III [74] (brown), and aSPECT [75] (orange).

4.6. Space Missions

Another way to determine neutron lifetime is to measure neutrons from the cosmic ray spallation of planets' and moons' surfaces (and atmospheres). A measurement of this type was performed using the neutron spectrometer onboard NASA's spacecraft MESSENGER mission [78], which, upon gathering data from Mercury and Venus, yielded the result $\tau_n = 780 \pm 60 \pm 70$ s.

This detection method was later implemented by the Lunar Prospector mission [79] to study neutrons from cosmic ray spallation of the Moon, leading to the result $\tau_n = 887 \pm 14^{+7}_{-3}$ s. Although those numbers are not competitive with beam and bottle results, future missions should be able to improve the accuracy to $\sim$1 s.

4.7. Colliders

Finally, one can also look for indirect signs of neutron dark decay at colliders, namely for the heavy color triplet scalar Φ mediating the decay. If in Model 1, the couplings satisfy $|\lambda_q \lambda_\chi| \lesssim 10^{-4}$ or in Model 2, one has $|\lambda_q \lambda_{\tilde{\chi}} \lambda_\phi| \lesssim 10^{-4}$, then Φ would be accessible at the Large Hadron Collider (LHC).

The opportunities to search for the colored scalar Φ would be much more promising at the Future Circular Collider (FCC) [80]. With a center-of-mass energy on the order of 100 TeV, regions of parameter space with considerably larger values of λ_q and λ_χ would be within experimental reach.

5. Theoretical Developments

The neutron dark decay proposal in [35] initiated not just experimental but also intense theoretical investigations. Those included studying neutron dark decay implications for neutron stars, which revealed the necessity of extending Models 1 and 2 to comply with the observed neutron star masses. It was also shown that certain models with neutron dark decay are capable of explaining both the nature of dark matter and the origin of the matter–antimatter asymmetry of the Universe. Apart from that, novel experimental signatures of neutron dark decay models were proposed, arising from processes such as dark matter–neutron annihilation inside atoms or dark matter capture by atomic nuclei. Connections to other anomalies in particle physics were investigated as well. Finally, it was pointed out that not only the neutron but also other hadrons can undergo dark decays with interesting predictions for hyperon, charm, and B factories. We discuss those and other follow-up theoretical ideas below.

5.1. Neutron Star Masses

Neutron stars do not become unstable due to the presence of a dark decay channel for the neutron since, similarly to the standard Pauli blocking of neutron β decays by the degeneracy pressure of the protons and electrons, neutron dark decays are blocked by the degeneracy pressure caused by χ particles. Nevertheless, a neutron dark decay channel would soften the neutron star equation of state and result in smaller than observed neutron star masses [81–83]. In particular, within the framework of Models 1 and 2, the masses of neutron stars would not exceed $0.8\,M_\odot$, which is significantly below the $2\,M_\odot$ value for some of the observed neutron stars.

To solve this problem, the neutron star equation of state has to be made stiffer, which can be achieved by supplementing Models 1 and 2 with additional ingredients. In particular, neutron stars with $2\,M_\odot$ can exist in the presence of a neutron dark decay channel if strong repulsive self-interactions in the dark sector are introduced [81–83] or there are repulsive interactions between the dark matter particle and the neutron [84]. Interestingly, such self-interactions were proposed in the past to solve the ΛCDM cosmological model's small-scale structure problems [85].

5.2. Self-Interactions in the Dark Sector

Dark sector self-interactions can be introduced by adding a dark vector gauge boson. A model of this type was constructed in [86], where the dark gauge boson is a dark photon A' and the neutron dark decay channel is $n \to \chi\, A'$. The Lagrangian of Model 1 is supplemented with the terms

$$\mathcal{L}_1' \supset -\tfrac{1}{4}F'_{\mu\nu}F'^{\mu\nu} - \tfrac{1}{2}\,\delta\, F_{\mu\nu}F'^{\mu\nu}\,, \tag{38}$$

and the covariant derivative is modified to $D_\mu - ig' A'_\mu$, where g' is the gauge coupling. The interaction between χ and A' is governed by g' and produces repulsion between the χ particles. It was demonstrated in [86] that this model simultaneously accommodates $\mathrm{Br}(n \to \chi\, A') = 1\%$ and neutron stars with $2\,M_\odot$ for a wide range of δ and g' values. The particle χ can be a dark matter candidate; however, if thermally produced, it can account for only a small fraction of the dark matter in the Universe. This model can also be slightly extended to explain the matter–antimatter asymmetry of the Universe through low-scale baryogenesis [87].

It is also possible to build extensions of Model 2 which are consistent with all astrophysical constraints. One of such theories was constructed in [88] by augmenting the Model 2 Lagrangian with terms including a dark gauge boson Z_D, thus resulting in the following dark sector self-interactions,

$$\mathcal{L}_2' \supset g'\bar{\chi}\, \not{Z}_D \chi - i\, g' (\phi^* \partial_\mu \phi - \phi\, \partial_\mu \phi^*)\, Z_D^\mu\,. \tag{39}$$

It was shown in [88] that one can have $\mathrm{Br}(n \to \chi\, \phi) = 1\%$, the particle χ (if non-thermally produced) can account for all of the dark matter in the Universe, and the self-interactions, making the model consistent with the observed neutron star masses, also provide a solution to the missing satellite problem, the "too big to fail" problem, and the core vs. cusp problem.

In addition to constructing models of neutron dark decay with extra $\mathrm{U}(1)$ interactions, in [89], it was shown that the Standard Model can be extended by an $\mathrm{SU}(2)$ dark group, with the neutron dark decaying via $n \to \chi W'$ and χ constituting all of the thermally produced dark matter in the Universe.

5.3. Dark Matter–Neutron Repulsion

An alternative idea allowing for consistency with neutron star constraints is to postulate additional repulsive interactions between the dark matter χ and the neutron [84], which is achieved by extending the Lagrangian of Model 2 by

$$\mathcal{L}_2'' \supset \mu H^\dagger H \phi + g_\chi \bar{\chi} \chi \phi \,. \tag{40}$$

This introduces an effective coupling $g_n \bar{n} n \phi$ via the Higgs portal, modifying the neutron star equation of state and, despite of the presence of the neutron decay channel $n \to \chi \phi$, permitting neutron stars to have $2\,M_\odot$.

5.4. Stability of Hydrogen

It was pointed out in [43,90] that in the case of Model 1 with χ being the dark matter particle, i.e., $m_\chi < m_p + m_e = 938.783$ MeV, hydrogen becomes unstable with respect to the following dark decay channel,

$$\mathrm{H} \to \chi \nu_e \,. \tag{41}$$

The branching ratio for the radiative contribution to this process, $\mathrm{H} \to \chi \nu_e \gamma$, is constrained by Borexino data [43]. This leads to an additional constraint on the neutron dark decay channel $n \to \chi \gamma$ corresponding to the purple-shaded region in Figure 5, which is excluded at a high confidence level. This implies that the allowed range of dark matter masses with $\mathrm{Br}(n \to \chi \gamma) > 0.5\%$ is narrowed down to $m_\chi \gtrsim 938.5$ MeV.

5.5. Dark Matter Nuclear Capture

A new dark matter detection strategy is possible in models exhibiting the neutron dark decay channel $n \to \chi \gamma$. Since $B_\chi = 1$, the particle χ can be captured by atomic nuclei [91] because of the χ-neutron mixing. This process is most interesting when χ is a dark matter candidate, since then χ from the galactic halo can be captured by a nucleus in a detector. If the nucleus is (Z, A), the dark matter capture forms an excited nucleus $(Z, A+1)^*$, which subsequently de-excites by emitting one photon or a cascade of photons,

$$\chi + (Z, A) \;\to\; (Z, A+1)^* \;\to\; (Z, A+1) + \gamma_{\mathrm{cascade}} \,, \tag{42}$$

with energy related to the dark matter mass through

$$E_{\mathrm{cascade}} = S_n - (m_n - m_\chi) \,. \tag{43}$$

Here, S_n is the neutron separation energy for the nucleus $(Z, A+1)$. As a result, the energy of this cascade differs from the energy of a standard cascade (caused by neutron capture) by the mass difference $(m_n - m_\chi)$. This signature can be searched for in dark matter direct detection experiments, e.g., PandaX [92], XENONnT [93], and LUX-Zeplin [94], as well as large volume neutrino experiments, such as the future Deep Underground Neutrino Experiment (DUNE) [95]. The analysis in [91] reveals that the discovery prospects are encouraging.

Dark matter nuclear absorption signals were further studied in [96]. It was shown that data from deep underground detectors such as SNO and Borexino place strong limits in a wide range of parameter space. Other possible signatures were also considered, including neutrons “shining through walls” at spallation sources, reactors, and the disappearance of UCN.

5.6. Dark Matter–Neutron Annihilation

The particle χ produced in neutron dark decay need not necessarily be the dark matter particle, but it can rather be the antiparticle of dark matter. This would imply that the dark matter in the galactic halo carries baryon number $B_{\bar{\chi}} = -1$, leading to spectacular signatures in direct detection experiments [97,98] (see also more general work in [99,100]), since dark matter can annihilate with nucleons inside nuclei via the following processes,

- Model 1: $\bar{\chi} + n \to \gamma + \text{meson(s)};$
- Model 2: $\bar{\chi} + n \to \phi + \text{meson(s)}.$

Here, the final state mesons experience very different kinematics than in standard nucleon decay considerations, which could be discovered in experiments such as Super-Kamiokande [101] and DUNE [95]. It was shown [97,98] that this scenario (when χ is the antiparticle of dark matter) is experimentally excluded in the case of Model 1, but there exists a large parameter range for which it remains viable in the case of Model 2.

5.7. Hadron Dark Decays

The intermediate particles in neutron dark decay do not have to couple exclusively to first-generation quarks. Allowing for nonzero interactions with quarks of different flavors (in this case, $\text{Br}(n \to \chi\,\gamma) \lesssim 10^{-6}$ [102] due to the stringent flavor constraints from kaon mixing, but the dark decay $n \to \chi\,\phi$ remains unconstrained) leads to the possibility of hadrons other than the neutron undergoing dark decays. This idea was first applied to neutral kaons and B-mesons in [103] and later extended to other heavy hadrons in [104], leading to apparent baryon number violation signals searchable not only in Super-K and DUNE but also in charm and B factories.

If the color triplet scalar Φ in Models 1 and 2 couples also to strange quarks, this leads to dark decays of hyperons Λ, Σ, and Ξ. This scenario was investigated in great detail in [105] and, in the case of the Λ baryon, gives rise to the following dark decay channels,

$$\Lambda \to \chi\,\phi\,, \quad \Lambda \to \pi^0\chi\,, \quad \Lambda \to \chi\,\gamma\,. \tag{44}$$

Building up on novel calculations of matrix elements relevant for hyperon dark decays, the expected rates at hyperon factories, such as BESIII [106] and LHCb, were determined. It was demonstrated that prospects for the discovery of such hyperon dark decays are promising.

5.8. Neutron–Mirror Neutron Oscillations

It was suggested in [107] that the neutron lifetime discrepancy is a result of neutron-mirror neutron oscillations. However, as was pointed out in [108], to make this model consistent with the experiment, an extreme breaking of the Z_2 symmetry between the Standard Model and its mirror copy is necessary. A somewhat related proposal in [109] states that in the neutron–mirror neutron oscillation model, the neutron dark decay can be mediated by nonperturbative effects.

Additional constraints on the neutron–mirror neutron oscillation interpretation were derived in [110] from neutron star internal heating, which occurs when neutrons in the core of a neutron star are converted to mirror neutrons during collisions, and the vacancies left behind in the nucleon Fermi seas are refilled by more energetic nucleons. The corresponding limits are competitive with those from laboratory searches for neutron–mirror neutron transitions, and they are applicable to a much wider range of mass splittings. This new heating mechanism can be probed by upcoming ultraviolet, optical, and infrared telescopes.

It was also proposed that the neutron lifetime anomaly can be resolved by neutron–mirror neutron oscillations intensifying in the presence of a magnetic field in beam experiments [90], but this was later experimentally excluded in [111].

5.9. Other Theoretical Progress

A qualitatively different scenario, not requiring dark matter to have self-repulsive interactions, was proposed in [112], where it was shown that there can exist a neutron decay channel to three dark matter particles, $n \to \chi\chi\chi$. Although a UV complete model has not been constructed, an effective four-fermion operator involving the Dirac spinor $\Psi = (\chi_L, \bar{\chi}_R)$ was written down,

$$\mathcal{L}_{\rm eff}^{\dim 6} \sim \frac{(\overline{\Psi}^c \Gamma \Psi)(\bar{n}^c \Gamma \Psi)}{\Lambda^2} , \tag{45}$$

where, e.g., $\Gamma = \gamma_\mu g_V(1 + \lambda\gamma_5)$. It was demonstrated that such a neutron dark decay channel is compatible with all experimental bounds, including neutron star constraints. This was further confirmed by a more detailed analysis in [113].

In [114], it was proposed that Model 1 with an extra dark fermion ψ can explain the excess of electron recoil events recorded by XENON1T [115], but that anomaly disappeared with more data collected by the XENONnT detector [93]. In [116], novel neutron dark decay channels were proposed involving an intermediate new boson, which could be as light as 17 MeV and provide a solution also to the ^{8}Be nuclear transitions anomaly [117,118].

Alternative explanations of the neutron lifetime discrepancy include a large Fierz interference term [119] and the quantum Zeno effect [120]. The suggestion was also put forward that in beam experiments, there is an unaccounted for loss of protons due to their collisions with the residual gas molecules in the quasi-Penning trap or other processes [121–123].

Finally, models of neutron dark decay have recently been shown to fit into the framework of asymmetric dark matter. This becomes possible if there are two or more types of dark matter particles and one of them has a mass below that of the neutron. Intriguingly, such models, e.g., the one based on the gauge group $SU(4) \times SU(2)_L \times U(1)_X \times SU(2)_\ell$ [124], can be probed with future gravitational wave experiments.

6. Conclusions

The neutron is one of the basic constituents of matter, and it is indispensable for the existence of complex atomic nuclei. Despite being studied throughout the last ninety years, the precise value of its lifetime is still an open question with beam and bottle experiments providing different results. Knowing the value of the neutron lifetime is important since it serves as an input for Big Bang nucleosynthesis calculations, directly affecting the primordial helium abundance. It also provides a clean test of the unitarity of the CKM matrix uninfluenced by nuclear structure effects.

It was demonstrated that the neutron lifetime discrepancy between beam and bottle experiments can be explained if the neutron exhibits a beyond-Standard-Model decay channel with a branching ratio of 1%. Concrete particle physics models accommodating such a neutron dark decay channel were constructed and shown to be consistent with all experiments and observations. Many of those models also provide answers to other outstanding questions in particle physics, e.g., concerning the nature of dark matter and the origin of the matter–antimatter asymmetry of the Universe.

The neutron dark decay creates a portal between the visible sector and the dark sector. As demonstrated in the original proposal and the follow-up literature, it predicts novel signatures in various experiments across many fields: nuclear physics (UCN, nuclear decays), dark matter direct detection (PandaX, XENONnT, LUX-Zeplin), neutrinos (Super-K, DUNE), colliders (LHC), and hyperon, charm, and B meson factories (Belle II, BESIII, LHCb). If any of the expected signals are discovered, pinning down the details of the dark decay channel will foster a close collaboration between different groups, bringing together the particle and nuclear physics communities.

It is worth realizing that even if the beam and bottle results converge in the future, neutron dark decays with smaller branching ratios will still be an intriguing possibility to consider, enabling us to probe the uncharted parameter space of the dark matter sector.

Funding: This work was funded by the National Science Foundation under Grant No. PHY-2213144.

Data Availability Statement: No new data were created or analyzed in this study. Data sharing is not applicable to this article.

Acknowledgments: The author is very grateful to Benjamín Grinstein for discussions and past collaboration.

Conflicts of Interest: The author declares no conflict of interest.

References

1. Thomson, J.J. Cathode Rays. *Philos. Mag.* **1897**, *44*, 293–316. [CrossRef]
2. Rutherford, E. Collision of α Particles with Light Atoms. IV. An Anomalous Effect in Nitrogen. *Philos. Mag. Ser. 6* **1919**, *37*, 581–587. [CrossRef]
3. Joliot-Curie, I.; Joliot-Curie, F. Emission de Protons de Grande Vitesse par les Substances Hydrogenees sous l'Influence des Rayons γ Tres Penetrants [Emission of High-Speed Protons by Hydrogenated Substances under the Influence of Very Penetrating γ-Rays]. *C. R. Seances L'Academie Sci.* **1932**, *194*, 273.
4. Chadwick, J. The Existence of a Neutron. *Proc. R. Soc. Lond. Ser.* **1932**, *136*, 692–708. [CrossRef]
5. Joliot-Curie, I.; Joliot-Curie, F. Mass of the Neutron. *Nature* **1934**, *133*, 721. [CrossRef]
6. Bales, M.J.; Alarcon, R.; Bass, C.D.; Beise, E.J.; Breuer, H.; Byrne, J.; Chupp, T.E.; Coakley, K.J.; Cooper, R.L.; Dewey, M.S.; et al. Precision Measurement of the Radiative β Decay of the Free Neutron. *Phys. Rev. Lett.* **2016**, *116*, 242501. [CrossRef]
7. Faber, M.; Ivanov, A.N.; Ivanova, V.A.; Marton, J.; Pitschmann, M.; Serebrov, A.P.; Troitskaya, N.I.; Wellenzohn, M. On Continuum-State and Bound-State Beta Decay Rates of the Neutron. *Phys. Rev. C* **2009**, *80*, 035503. [CrossRef]
8. Glashow, S.L. Partial Symmetries of Weak Interactions. *Nucl. Phys.* **1961**, *22*, 579–588. [CrossRef]
9. Higgs, P.W. Broken Symmetries and the Masses of Gauge Bosons. *Phys. Rev. Lett.* **1964**, *13*, 508–509. [CrossRef]
10. Englert, F.; Brout, R. Broken Symmetry and the Mass of Gauge Vector Mesons. *Phys. Rev. Lett.* **1964**, *13*, 321–323. [CrossRef]
11. Weinberg, S. A Model of Leptons. *Phys. Rev. Lett.* **1967**, *19*, 1264–1266. [CrossRef]
12. Salam, A. Weak and Electromagnetic Interactions. *Conf. Proc. C* **1968**, *680519*, 367–377.
13. Fritzsch, H.; Gell-Mann, M.; Leutwyler, H. Advantages of the Color Octet Gluon Picture. *Phys. Lett. B* **1973**, *47*, 365–368. [CrossRef]
14. Gross, D.J.; Wilczek, F. Ultraviolet Behavior of Nonabelian Gauge Theories. *Phys. Rev. Lett.* **1973**, *30*, 1343–1346. [CrossRef]
15. Politzer, H.D. Reliable Perturbative Results for Strong Interactions? *Phys. Rev. Lett.* **1973**, *30*, 1346–1349. [CrossRef]
16. Marciano, W.J.; Sirlin, A. Improved Calculation of Electroweak Radiative Corrections and the Value of V_{ud}. *Phys. Rev. Lett.* **2006**, *96*, 032002. [CrossRef]
17. Czarnecki, A.; Marciano, W.J.; Sirlin, A. Neutron Lifetime and Axial Coupling Connection. *Phys. Rev. Lett.* **2018**, *120*, 202002. [CrossRef]
18. Hardy, J.C.; Towner, I.S. Superallowed $0^+ \to 0^+$ Nuclear β Decays: 2014 Critical Survey, with Precise Results for V_{ud} and CKM Unitarity. *Phys. Rev. C* **2015**, *91*, 025501. [CrossRef]
19. Workman, R.L. et al. [Particle Data Group] Review of Particle Physics. *Prog. Theor. Exp. Phys.* **2022**, *2022*, 083C01. [CrossRef]
20. Chang, C.C.; Nicholson, A.N.; Rinaldi, E.; Berkowitz, E.; Garron, N.; Brantley, D.A.; Monge-Camacho, H.; Monahan, C.J.; Bouchard, C.; Clark, M.A.; et al. A Per-Cent-Level Determination of the Nucleon Axial Coupling from Quantum Chromodynamics. *Nature* **2018**, *558*, 91–94. [CrossRef]
21. Dubbers, D.; Schmidt, M.G. The Neutron and its Role in Cosmology and Particle Physics. *Rev. Mod. Phys.* **2011**, *83*, 1111–1171. [CrossRef]
22. Wietfeldt, F.E.; Greene, G.L. The Neutron Lifetime. *Rev. Mod. Phys.* **2011**, *83*, 1173–1192. [CrossRef]
23. Byrne, J.; Dawber, P.G. A Revised Value for the Neutron Lifetime Measured Using a Penning Trap. *Europhys. Lett.* **1996**, *33*, 187. [CrossRef]
24. Nico, J.S.; Dewey, M.S.; Gilliam, D.M.; Wietfeldt, F.E.; Fei, X.; Snow, W.M.; Greene, G.L.; Pauwels, J.; Eykens, R.; Lamberty, A.; et al. Measurement of the Neutron Lifetime by Counting Trapped Protons in a Cold Neutron Beam. *Phys. Rev. C* **2005**, *71*, 055502. [CrossRef]
25. Yue, A.T.; Dewey, M.S.; Gilliam, D.M.; Greene, G.L.; Laptev, A.B.; Nico, J.S.; Snow, W.M.; Wietfeldt, F.E. Improved Determination of the Neutron Lifetime. *Phys. Rev. Lett.* **2013**, *111*, 222501. [CrossRef] [PubMed]
26. Hirota, K.; Ichikawa, G.; Ieki, S.; Ino, T.; Iwashita, Y.; Kitaguchi, M.; Kitahara, R.; Koga, J.; Mishima, K.; Mogi, T.; et al. Neutron Lifetime Measurement with Pulsed Cold Neutrons. *Prog. Theor. Exp. Phys.* **2020**, *2020*, 123C02. [CrossRef]
27. Serebrov, A.; Varlamov, V.; Kharitonov, A.; Fomin, A.; Pokotilovski, Y.; Geltenbort, P.; Butterworth, J.; Krasnoschekova, I.; Lasakov, M.; Tal'daev, R.; et al. Measurement of the Neutron Lifetime Using a Gravitational Trap and a Low-Temperature Fomblin Coating. *Phys. Lett. B* **2005**, *605*, 72–78. [CrossRef]
28. Pichlmaier, A.; Varlamov, V.; Schreckenbach, K.; Geltenbort, P. Neutron Lifetime Measurement with the UCN Trap-in-Trap MAMBO II. *Phys. Lett. B* **2010**, *693*, 221–226. [CrossRef]

29. Steyerl, A.; Pendlebury, J.M.; Kaufman, C.; Malik, S.S.; Desai, A.M. Quasielastic Scattering in the Interaction of Ultracold Neutrons with a Liquid Wall and Application in a Reanalysis of the Mambo I Neutron Lifetime Experiment. *Phys. Rev. C* **2012**, *85*, 065503. [CrossRef]
30. Arzumanov, S.; Bondarenko, L.; Chernyavsky, S.; Geltenbort, P.; Morozov, V.; Nesvizhevsky, V.V.; Panin, Y.; Strepetov, A. A Measurement of the Neutron Lifetime Using the Method of Storage of Ultracold Neutrons and Detection of Inelastically Up-Scattered Neutrons. *Phys. Lett. B* **2015**, *745*, 79–89. [CrossRef]
31. Serebrov, A.P.; Kolomensky, E.A.; Fomin, A.K.; Krasnoshchekova, I.A.; Vassiljev, A.V.; Prudnikov, D.M.; Shoka, I.V.; Chechkin, A.V.; Chaikovskiy, M.E.; Varlamov, V.E.; et al. Neutron Lifetime Measurements with a Large Gravitational Trap for Ultracold Neutrons. *Phys. Rev. C* **2018**, *97*, 055503. [CrossRef]
32. Pattie, R.W., Jr.; Callahan, N.B.; Cude-Woods, C.; Adamek, E.R.; Broussard, L.J.; Clayton, S.M.; Currie, S.A.; Dees, E.B.; Ding, X.; Zeck, B.A.; et al. Measurement of the Neutron Lifetime Using a Magneto-Gravitational Trap and In Situ Detection. *Science* **2018**, *360*, 627–632. [CrossRef] [PubMed]
33. Ezhov, V.F.; Andreev, A.Z.; Ban, G.; Bazarov, B.A.; Geltenbort, P.; Glushkov, A.G.; Knyazkov, V.A.; Kovrizhnykh, N.A.; Krygin, G.B.; Ryabov, V.L.; et al. Measurement of the Neutron Lifetime with Ultra-Cold Neutrons Stored in a Magneto-Gravitational Trap. *J. Exp. Theor. Phys. Lett.* **2018**, *107*, 671–675. [CrossRef]
34. Gonzalez, F.M.; Fries, E.M.; Cude-Woods, C.; Bailey, T.; Blatnik, M.; Broussard, L.J.; Callahan, N.B.; Choi, J.H.; Clayton, S.M.; Young, A.R.; et al. Improved Neutron Lifetime Measurement with UCNτ. *Phys. Rev. Lett.* **2021**, *127*, 162501. [CrossRef] [PubMed]
35. Fornal, B.; Grinstein, B. Dark Matter Interpretation of the Neutron Decay Anomaly. *Phys. Rev. Lett.* **2018**, *120*, 191801; Erratum in *Phys. Rev. Lett.* **2020**, *124*, 219901. [CrossRef] [PubMed]
36. Ahmed, S.N.; Anthony, A.E.; Beier, E.W.; Bellerive, A.; Biller, S.D.; Boger, J.; Boulay, M.G.; Bowler, M.G.; Bowles, T.J.; Brice, S.J.; et al. Constraints on Nucleon Decay via Invisible Modes from the Sudbury Neutrino Observatory. *Phys. Rev. Lett.* **2004**, *92*, 102004. [CrossRef]
37. Araki, T.; Enomoto, S.; Furuno, K.; Gando, Y.; Ichimura, K.; Ikeda, H.; Inoue, K.; Kishimoto, Y.; Koga, M.; Koseki, Y.; et al. Search for the Invisible Decay of Neutrons with KamLAND. *Phys. Rev. Lett.* **2006**, *96*, 101802. [CrossRef]
38. Pfutzner, M.; Riisager, K. Examining the Possibility to Observe Neutron Dark Decay in Nuclei. *Phys. Rev. C* **2018**, *97*, 042501. [CrossRef]
39. Tang, Z.; Blatnik, M.; Broussard, L.J.; Choi, J.H.; Clayton, S.M.; Cude-Woods, C.; Currie, S.; Fellers, D.E.; Fries, E.M.; Geltenbort, P.; et al. Search for the Neutron Decay $n \to X + \gamma$ where X is a Dark Matter Particle. *Phys. Rev. Lett.* **2018**, *121*, 022505. [CrossRef]
40. Aoki, Y.; Izubuchi, T.; Shintani, E.; Soni, A. Improved Lattice Computation of Proton Decay Matrix Elements. *Phys. Rev.* **2017**, *D96*, 014506. [CrossRef]
41. Gustafson, J.; Abe, K.; Haga, Y.; Hayato, Y.; Ikeda, M.; Iyogi, K.; Kameda, J.; Kishimoto, Y.; Miura, M.; Moriyama, S.; et al. Search for Dinucleon Decay into Pions at Super-Kamiokande. *Phys. Rev. D* **2015**, *91*, 072009, [CrossRef]
42. Abe, K.; Hayato, Y.; Iida, T.; Ishihara, K.; Kameda, J.; Koshio, Y.; Minamino, A.; Mitsuda, C.; Miura, M.; Moriyama, S.; et al. The Search for $n - \bar{n}$ Oscillation in Super-Kamiokande I. *Phys. Rev. D* **2015**, *91*, 072006, [CrossRef]
43. McKeen, D.; Pospelov, M. How Long Does the Hydrogen Atom Live? *arXiv* **2020**, arXiv:2003.02270.
44. Agostini, M.; Appel, S.; Bellini, G.; Benziger, J.; Bick, D.; Bonfini, G.; Bravo, D.; Caccianiga, B.; Calaprice, F.; Caminata, A.; et al. A Test of Electric Charge Conservation with Borexino. *Phys. Rev. Lett.* **2015**, *115*, 231802. [CrossRef] [PubMed]
45. McKeen, D.; Pospelov, M.; Raj, N. Cosmological and Astrophysical Probes of Dark Baryons. *Phys. Rev. D* **2021**, *103*, 115002, [CrossRef]
46. Sun, X.; Adamek, E.; Allgeier, B.; Blatnik, M.; Bowles, T.J.; Broussard, L.J.; Brown, M.A.-P.; Carr, R.; Clayton, S.; Cude-Woods, C.; et al. Search for Dark Matter Decay of the Free Neutron from the UCNA Experiment: $n \to \chi + e^+e^-$. *Phys. Rev. C* **2018**, *97*, 052501. [CrossRef]
47. Klopf, M.; Jericha, E.; Markisch, B.; Saul, H.; Soldner, T.; Abele, H. Constraints on the Dark Matter Interpretation $n \to \chi + e^+e^-$ of the Neutron Decay Anomaly with the PERKEO II Experiment. *Phys. Rev. Lett.* **2019**, *122*, 222503. [CrossRef]
48. Borge, M.J.G.; Fraile, L.M.; Fynbo, H.O.U.; Jonson, B.; Kirsebom, O.S.; Nilsson, T.; Nyman, G.; Possnert, G.; Riisager, K.; Tengblad, O. Rare βp decays in light nuclei. *J. Phys. Nucl. Part. Phys.* **2013**, *40*, 035109. [CrossRef]
49. Riisager, K.; Forstner, O.; Borge, M.J.G.; Briz, J.A.; Carmona-Gallardo, M.; Fraile, L.M.; Fynbo, H.O.U.; Giles, T.; Gottberg, A.; Heinz, A.; et al. $^{11}Be(\beta p)$, a Quasi-Free Neutron Decay? *Phys. Lett. B* **2014**, *732*, 305–308. [CrossRef]
50. Ejiri, H.; Vergados, J.D. Neutron Disappearance Inside the Nucleus. *J. Phys. G* **2019**, *46*, 025104. [CrossRef]
51. CERN-ISOLDE Schedule. 2018. Available online: https://isolde.web.cern.ch/isolde-schedule (accessed on 26 July 2020).
52. Ayyad, Y.; Olaizola, B.; Mittig, W.; Potel, G.; Zelevinsky, V.; Horoi, M.; Beceiro-Novo, S.; Alcorta, M.; Andreoiu, C.; Ahn, T.; et al. Direct Observation of Proton Emission in ^{11}Be. *Phys. Rev. Lett.* **2019**, *123*, 082501; Erratum in *Phys. Rev. Lett.* **2020**, *124*, 129902. [CrossRef] [PubMed]
53. Ayyad, Y.; Mittig, W.; Tang, T.; Olaizola, B.; Potel, G.; Rijal, N.; Watwood, N.; Alvarez-Pol, H.; Bazin, D.; Chen, J.; et al. Evidence of a Near-Threshold Resonance in ^{11}B Relevant to the β-Delayed Proton Emission of ^{11}Be. *Phys. Rev. Lett.* **2022**, *129*, 012501. [CrossRef] [PubMed]
54. Lopez-Saavedra, E.; Almaraz-Calderon, S.; Asher, B.W.; Baby, L.T.; Gerken, N.; Hanselman, K.; Kemper, K.W.; Kuchera, A.N.; Morelock, A.B.; Perello, J.F.; et al. Observation of a Near-Threshold Proton Resonance in ^{11}B. *Phys. Rev. Lett.* **2022**, *129*, 012502. [CrossRef] [PubMed]

55. Okolowicz, J.; Ploszajczak, M.; Nazarewicz, W. Convenient Location of a Near-Threshold Proton-Emitting Resonance in ^{11}B. *Phys. Rev. Lett.* **2020**, *124*, 042502. [CrossRef]
56. Anh, N.L.; Loc, B.M.; Auerbach, N.; Zelevinsky, V. Single-Particle Properties of the Near-Threshold Proton-Emitting Resonance in ^{11}B. *Phys. Rev. C* **2022**, *106*, L051302. [CrossRef]
57. Riisager, K.; Borge, M.J.G.; Briz, J.A.; Carmona-Gallardo, M.; Forstner, O.; Fraile, L.M.; Fynbo, H.O.U.; Camacho, A.G.; Johansen, J.G.; Jonson, B.; et al. Search for Beta-Delayed Proton Emission from ^{11}Be. *Eur. Phys. J. A* **2020**, *56*, 100. [CrossRef]
58. Le Joubioux, M.; Savajols, H.; Mittig, W.; Fléchard, X.; Penionzhkevich, Y.E.; Ackermann, D.; Borcea, C.; Caceres, L.; Delahaye, P.; Didierjean, F.; et al. Is There a Dark Decay of Neutrons in ^{6}He? *arXiv* **2023**, arXiv:2308.16536.
59. Anthony, D.; Buchmann, L.; Bergbusch, P.; D'Auria, J.M.; Dombsky, M.; Giesen, U.; Jackson, K.P.; King, J.D.; Powell, J.; Barker, F.C. β-Delayed Deuteron Emission from ^{6}He. *Phys. Rev. C* **2002**, *65*, 034310. [CrossRef]
60. Raabe, R.; Büscher, J.; Ponsaers, J.; Aksouh, F.; Huyse, M.; Ivanov, O.; Lesher, S.R.; Mukha, I.; Pauwels, D.; Sawicka, M.; et al. Measurement of the Branching Ratio of the ^{6}He β-Decay Channel into the $\alpha + d$ Continuum. *Phys. Rev. C* **2009**, *80*, 054307. [CrossRef]
61. Pfutzner, M.; Dominik, W.; Janas, Z.; Mazzocchi, C.; Pomorski, M.; Bezbakh, A.A.; Borge, M.J.G.; Chrapkiewicz, K.; Chudoba, V.; Frederickx, R.; et al. β Decay of ^{6}He into the $\alpha + d$ Continuum. *Phys. Rev. C* **2015**, *92*, 014316. [CrossRef]
62. Dewey, M.; Coakley, K.; Gilliam, D.; Greene, G.; Laptev, A.; Nico, J.; Snow, W.; Wietfeldt, F.; Yue, A. Prospects for a New Cold Neutron Beam Measurement of the Neutron Lifetime. *Nucl. Instrum. Methods A* **2009**, *611*, 189. [CrossRef]
63. Hoogerheide, S.F.; Caylor, J.; Adamek, E.R.; Anderson, E.S.; Biswas, R.; Chavali, S.M.; Crawford, B.; DeAngelis, C.; Dewey, M.S.; Yue, A.T.; et al. Progress on the BL2 Beam Measurement of the Neutron Lifetime. *EPJ Web Conf.* **2019**, *219*, 03002. [CrossRef]
64. Nagakura, N.; Hirota, K.; Ieki, S.; Ino, T.; Iwashita, Y.; Kitaguchi, M.; Kitahara, R.; Mishima, K.; Morishita, A.; Oide, H.; et al. Precise Neutron Lifetime Experiment Using Pulsed Neutron Beams at J-PARC. *arXiv* **2017**, arXiv:1702.03099. [CrossRef]
65. Nagakura, N.; Hirota, K.; Ieki, S.; Ino, T.; Iwashita, Y.; Kitaguchi, M.; Kitahara, R.; Koga, J.; Mishima, K.; Morishita, A.; et al. New Project for Precise Neutron Lifetime Measurement at J-PARC. *EPJ Web Conf.* **2019**, *219*, 03003. [CrossRef]
66. Sumi, N.; Hirota, K.; Ichikawa, G.; Ino, T.; Iwashita, Y.; Kajiwara, S.; Kato, Y.; Kitaguchi, M.; Mishima, K.; Morikawa, K.; et al. Precise Neutron Lifetime Measurement Using Pulsed Neutron Beams at J-PARC. *JPS Conf. Proc.* **2021**, *33*, 011056. [CrossRef]
67. Nelsen, A.W.; Ballantyne, E.G.; Calvert, R.E.; Crawford, C.B.; Greene, G.L.; Vickers, S.E.; Wietfeldt, F.E. Geometric Optimization of a Neutron Detector for In-Flight Measurement of the Neutron Lifetime. *arXiv* **2020**, arXiv:2010.11250.
68. Fomin, N.; BL3 Collaboration. BL3: Next Generation Beam Experiment to Measure the Neutron Lifetime. In Proceedings of the APS April Meeting Abstracts, Virtual, 16–19 April 2021; Volume 2021, p. T11.008.
69. Wietfeldt, F.; BL3 Collaboration Team. The BL3 Beam Neutron Lifetime Experiment. In Proceedings of the APS April Meeting Abstracts, New York, NY, USA, 9–12 April 2022; Volume 2022, p. T12.004.
70. Fry, J. BL3: The Next Generation Neutron Lifetime Measurement Using the Beam Method. In Proceedings of the Talk at the APS Southeastern Section Meeting 2022, Oxford, MS, USA, 3–5 November 2022. Available online: https://meetings.aps.org/Meeting/SES22/Session/K03.3 (accessed on 27 June 2023).
71. Fornal, B.; Grinstein, B. Dark Side of the Neutron? *EPJ Web Conf.* **2019**, *219*, 05005. [CrossRef]
72. Tang, Z.; Cude-Woods, C.; Clayton, S.; Morris, C.; Ito, T.; Makela, M.; Saunders, A.; Choi, J.H.; Lambert, J.; Liu, C.-Y.; et al. Ultra-Cold Neutron Measurement of Proton Branching Ratio in Neutron Beta Decay (UCNProBe). In Proceedings of the Talk at the APS Meeting 2019, Denver, CO, USA, 13–16 April 2019. Available online: http://meetings.aps.org/Meeting/APR19/Session/H14.5 (accessed on 27 June 2023).
73. Hassan, M.; Floyd, N.; Tang, Z.; UCNProBe Team. The Current Status of the UCNProBe Experiment. In Proceedings of the APS Division of Nuclear Physics Meeting Abstracts, Virtual, 11–14 October 2021; Volume 2021, p. QJ.008.
74. Markisch, B.; Mest, H.; Saul, H.; Wang, X.; Abele, H.; Dubbers, D.; Klopf, M.; Petoukhov, A.; Roick, C.; Soldner, T.; et al. Measurement of the Weak Axial-Vector Coupling Constant in the Decay of Free Neutrons Using a Pulsed Cold Neutron Beam. *Phys. Rev. Lett.* **2019**, *122*, 242501. [CrossRef]
75. Beck, M.; Ayala Guardia, F.; Borg, M.; Kahlenberg, J.; Muñoz Horta, R.; Schmidt, C.; Wunderle, A.; Heil, W.; Maisonobe, R.; Simson, M.; et al. Improved Determination of the β-$\overline{\nu}_e$ Angular Correlation Coefficient a in Free Neutron Decay with the $aSPECT$ Spectrometer. *Phys. Rev. C* **2020**, *101*, 055506. [CrossRef]
76. Hassan, M.T.; Byron, W.A.; Darius, G.; DeAngelis, C.; Wietfeldt, F.E.; Collett, B.; Jones, G.L.; Komives, A.; Noid, G.; Stephenson, E.J.; et al. Measurement of the Neutron Decay Electron-Antineutrino Angular Correlation by the aCORN Experiment. *Phys. Rev. C* **2021**, *103*, 045502. [CrossRef]
77. Dubbers, D.; Markisch, B. Precise Measurements of the Decay of Free Neutrons. *Ann. Rev. Nucl. Part. Sci.* **2021**, *71*, 139–163. [CrossRef]
78. Wilson, J.T.; Lawrence, D.J.; Peplowski, P.N.; Eke, V.R.; Kegerreis, J.A. Space-Based Measurement of the Neutron Lifetime Using Data from the Neutron Spectrometer on NASA's MESSENGER Mission. *Phys. Rev. Res.* **2020**, *2*, 023316. [CrossRef]
79. Wilson, J.T.; Lawrence, D.J.; Peplowski, P.N.; Eke, V.R.; Kegerreis, J.A. Measurement of the Free Neutron Lifetime Using the Neutron Spectrometer on NASA's Lunar Prospector Mission. *Phys. Rev. C* **2021**, *104*, 045501. [CrossRef]
80. Abada, A.; Abbrescia, M.; AbdusSalam, S.S.; Abdyukhanov, I.; Fernandez, J.A.; Abramov, A.; Aburaia, M.; Acar, A.O.; Adzic, P.R.; Agrawal, P.; et al. FCC Physics Opportunities: Future Circular Collider Conceptual Design Report Volume 1. *Eur. Phys. J. C* **2019**, *79*, 474. [CrossRef]

81. Baym, G.; Beck, D.H.; Geltenbort, P.; Shelton, J. Testing Dark Decays of Baryons in Neutron Stars. *Phys. Rev. Lett.* **2018**, *121*, 061801. [CrossRef]
82. McKeen, D.; Nelson, A.E.; Reddy, S.; Zhou, D. Neutron Stars Exclude Light Dark Baryons. *Phys. Rev. Lett.* **2018**, *121*, 061802. [CrossRef]
83. Motta, T.F.; Guichon, P.A.M.; Thomas, A.W. Implications of Neutron Star Properties for the Existence of Light Dark Matter. *J. Phys. G* **2018**, *45*, 05LT01. [CrossRef]
84. Grinstein, B.; Kouvaris, C.; Nielsen, N.G. Neutron Star Stability in Light of the Neutron Decay Anomaly. *Phys. Rev. Lett.* **2019**, *123*, 091601. [CrossRef]
85. Spergel, D.N.; Steinhardt, P.J. Observational Evidence for Self-Interacting Cold Dark Matter. *Phys. Rev. Lett.* **2000**, *84*, 3760–3763. [CrossRef]
86. Cline, J.M.; Cornell, J.M. Dark Decay of the Neutron. *J. High Energy Phys.* **2018**, *07*, 081, [CrossRef]
87. Bringmann, T.; Cline, J.M.; Cornell, J.M. Baryogenesis from Neutron–Dark Matter Oscillations. *Phys. Rev. D* **2019**, *99*, 035024. [CrossRef]
88. Karananas, G.K.; Kassiteridis, A. Small-Scale Structure from Neutron Dark Decay. *J. Cosmol. Astropart. Phys.* **2018**, *09*, 036, [CrossRef]
89. Elahi, F.; Mohammadi Najafabadi, M. Neutron Decay to a Non-Abelian Dark Sector. *Phys. Rev.* **2020**, *102*, 035011. [CrossRef]
90. Berezhiani, Z. Neutron Lifetime Puzzle and Neutron—Mirror Neutron Oscillation. *Eur. Phys. J. C* **2019**, *79*, 484. [CrossRef]
91. Fornal, B.; Grinstein, B.; Zhao, Y. Dark Matter Capture by Atomic Nuclei. *Phys. Lett. B* **2020**, *811*, 135869. [CrossRef]
92. Cao, X.; Chen, X.; Chen, Y.; Cui, X.; Fang, D.; Fu, C.; Giboni, K.L.; Gong, H.; Guo, G.; He, M.; et al. PandaX: A Liquid Xenon Dark Matter Experiment at CJPL. *Sci. China Phys. Mech. Astron.* **2014**, *57*, 1476–1494. [CrossRef]
93. Aprile, E.; Abe, K.; Agostini, F.; Ahmed Maouloud, S.; Althueser, L.; Andrieu, B.; Angelino, E.; Angevaare, J.R.; Antochi, V.C.; Antón Martin, D.; et al. Search for New Physics in Electronic Recoil Data from XENONnT. *Phys. Rev. Lett.* **2022**, *129*, 161805. [CrossRef]
94. Murphy, A. et al. [The LUX-ZEPLIN (LZ) Collaboration] The LUX-ZEPLIN (LZ) Experiment. *Nucl. Instrum. Methods A* **2020**, *953*, 163047. [CrossRef]
95. Abi, B.; Acciarri, R.; Acero, M.A.; Adamov, G.; Adams, D.; Adinolfi, M.; Ahmad, Z.; Ahmed, J.; Alion, T.; Monsalve, S.A.; et al. Deep Underground Neutrino Experiment (DUNE), Far Detector Technical Design Report. *arXiv* **2020**, arXiv:2002.03005.
96. Hostert, M.; McKeen, D.; Pospelov, M.; Raj, N. Dark Sectors in Neutron-Shining-Through-a-Wall and Nuclear-Absorption Signals. *Phys. Rev. D* **2023**, *107*, 075034. [CrossRef]
97. Jin, M.; Gao, Y. Nucleon—Light Dark Matter Annihilation through Baryon Number Violation. *Phys. Rev. D* **2018**, *98*, 075026. [CrossRef]
98. Keung, W.Y.; Marfatia, D.; Tseng, P.Y. Annihilation Signatures of Neutron Dark Decay Models in Neutron Oscillation and Proton Decay Searches. *J. High Energy Phys.* **2019**, *09*, 053. [CrossRef]
99. Davoudiasl, H.; Morrissey, D.E.; Sigurdson, K.; Tulin, S. Hylogenesis: A Unified Origin for Baryonic Visible Matter and Antibaryonic Dark Matter. *Phys. Rev. Lett.* **2010**, *105*, 211304. [CrossRef] [PubMed]
100. Davoudiasl, H.; Morrissey, D.E.; Sigurdson, K.; Tulin, S. Baryon Destruction by Asymmetric Dark Matter. *Phys. Rev. D* **2011**, *84*, 096008. [CrossRef]
101. Fukuda, S.; Fukuda, Y.; Hayakawa, T.; Ichihara, E.; Ishitsuka, M.; Itow, Y.; Kajita, T.; Kameda, J.; Kaneyuki, K.; Kasuga, S.; et al. The Super-Kamiokande Detector. *Nucl. Instrum. Methods A* **2003**, *501*, 418–462. [CrossRef]
102. Fajfer, S.; Susic, D. Colored Scalar Mediated Nucleon Decays to an Invisible Fermion. *Phys. Rev. D* **2021**, *103*, 055012. [CrossRef]
103. Barducci, D.; Fabbrichesi, M.; Gabrielli, E. Neutral Hadrons Disappearing into the Darkness. *Phys. Rev. D* **2018**, *98*, 035049. [CrossRef]
104. Heeck, J. Light Particles with Baryon and Lepton Numbers. *Phys. Lett. B* **2021**, *813*, 136043. [CrossRef]
105. Alonso-Alvarez, G.; Elor, G.; Escudero, M.; Fornal, B.; Grinstein, B.; Martin Camalich, J. Strange Physics of Dark Baryons. *Phys. Rev. D* **2022**, *105*, 115005. [CrossRef]
106. Ablikim, M.; Achasov, M.N.; Adlarson, P.; Ahmed, S.; Albrecht, M.; Aliberti, R.; Amoroso, A.; An, M.R.; An, Q.; Bai, X.H.; et al. Search for Invisible Decays of the Λ Baryon. *Phys. Rev. D* **2022**, *105*, L071101. [CrossRef]
107. Berezhiani, Z. Neutron Lifetime and Dark Decay of the Neutron and Hydrogen. *Lett. High Energy Phys.* **2019**, *2*, 118, [CrossRef]
108. Fornal, B.; Grinstein, B. Comment on "Neutron lifetime and dark decay of the neutron and hydrogen". *arXiv* **2019**, arXiv:1902.08975.
109. Tan, W. Neutron Oscillations for Solving Neutron Lifetime and Dark Matter Puzzles. *Phys. Lett. B* **2019**, *797*, 134921. [CrossRef]
110. McKeen, D.; Pospelov, M.; Raj, N. Neutron Star Internal Heating Constraints on Mirror Matter. *Phys. Rev. Lett.* **2021**, *127*, 061805. [CrossRef] [PubMed]
111. Broussard, L.J.; Barrow, J.L.; DeBeer-Schmitt, L.; Dennis, T.; Fitzsimmons, M.R.; Frost, M.J.; Gilbert, C.E.; Gonzalez, F.M.; Heilbronn, L.; Iverson, E.B.; et al. Experimental Search for Neutron to Mirror Neutron Oscillations as an Explanation of the Neutron Lifetime Anomaly. *Phys. Rev. Lett.* **2022**, *128*, 212503. [CrossRef] [PubMed]
112. Strumia, A. Dark Matter Interpretation of the Neutron Decay Anomaly. *J. High Energy Phys.* **2022**, *2*, 067. [CrossRef]
113. Husain, W.; Thomas, A.W. Novel Neutron Decay Mode Inside Neutron Stars. *J. Phys. G* **2023**, *50*, 015202. [CrossRef]
114. McKeen, D.; Pospelov, M.; Raj, N. Hydrogen Portal to Exotic Radioactivity. *Phys. Rev. Lett.* **2020**, *125*, 231803. [CrossRef]

115. Aprile, E.; Aalbers, J.; Agostini, F.; Alfonsi, M.; Althueser, L.; Amaro, F.D.; Antochi, V.C.; Angelino, E.; Angevaare, J.R.; Arneodo, F.; et al. Observation of Excess Electronic Recoil Events in XENON1T. *arXiv* **2020**, arXiv:2006.09721.
116. Tien Du, P.; Ai Viet, N.; Van Dat, N. Decay of Neutron with Participation of the Light Vector Boson X17. *J. Phys. Conf. Ser.* **2020**, *1506*, 012004. [CrossRef]
117. Krasznahorkay, A.J.; Csatlós, M.; Csige, L.; Gácsi, Z.; Gulyás, J.; Hunyadi, M.; Kuti, I.; Nyakó, B.M.; Stuhl, L.; Timár, J.; et al. Observation of Anomalous Internal Pair Creation in ^{8}Be: A Possible Indication of a Light, Neutral Boson. *Phys. Rev. Lett.* **2016**, *116*, 042501. [CrossRef] [PubMed]
118. Feng, J.L.; Fornal, B.; Galon, I.; Gardner, S.; Smolinsky, J.; Tait, T.M.P.; Tanedo, P. Protophobic Fifth-Force Interpretation of the Observed Anomaly in ^{8}Be Nuclear Transitions. *Phys. Rev. Lett.* **2016**, *117*, 071803. [CrossRef] [PubMed]
119. Ivanov, A.N.; Hollwieser, R.; Troitskaya, N.I.; Wellenzohn, M.; Berdnikov, Y.A. Neutron Dark Matter Decays. *arXiv* **2018**, arXiv:1806.10107.
120. Giacosa, F.; Pagliara, G. Measurement of the Neutron Lifetime and Inverse Quantum Zeno Effect. *Phys. Rev. D* **2020**, *101*, 056003. [CrossRef]
121. Byrne, J.; Worcester, D.L. The Neutron Lifetime Anomaly and Charge Exchange Collisions of Trapped Protons. *J. Phys. G* **2019**, *46*, 085001. [CrossRef]
122. Serebrov, A.P.; Chaikovskii, M.E.; Klyushnikov, G.N.; Zherebtsov, O.M.; Chechkin, A.V. Search for Explanation of the Neutron Lifetime Anomaly. *Phys. Rev. D* **2021**, *103*, 074010. [CrossRef]
123. Byrne, J.; Worcester, D.L. The Neutron Lifetime Anomaly: Analysis of Charge Exchange and Molecular Reactions in a Proton Trap. *Eur. Phys. J. A* **2022**, *58*, 151. [CrossRef]
124. Fornal, B.; Garcia, K.; Pierre, E. Testing Unification and Dark Matter with Gravitational Waves. *Phys. Rev. D* **2023**, *108*, 055022. [CrossRef]